Beam trajectory control of the future Compact Linear Collider

G. Balik, A. Badel, B. Bolzon, L. Brunetti, B. Caron, G. Deleglise, A. Jérémie, R. Le Breton, J. Lottin, L. Pacquet

BEAM TRAJECTORY CONTROL OF THE FUTURE COMPACT LINEAR COLLIDER

G. Balik
LAPP, Université de Savoie, CNRS/IN2P3, Annecy-le-Vieux, France
gael.balik@lapp.in2p3.fr

A. Badel[3], B. Bolzon[2], L. Brunetti[1], B. Caron[3], G. Deleglise[1], A. Jeremie[1], R. Le breton[3], J. Lottin[3], L. Pacquet[1]
1: LAPP, Université de Savoie, CNRS/IN2P3, Annecy-le-Vieux, France
2: CERN-European Organization for Nuclear Research, Geneva, Switzerland
3: SYMME-Polytech Annecy Chambéry - Université de Savoie - Annecy-le-Vieux France

Keywords: Adaptive algorithm - Disturbance rejection - Least-squares algorithm - Optical feedback - Parameter optimization - Vibration control

Abstract: The future Compact LInear Collider (CLIC) currently under design at CERN (European Organization for Nuclear Research) would create high-energy particle collisions between electrons and positrons, and provide a tool for scientists to address many of the most compelling questions about the fundamental nature of matter, energy, space and time. In accelerating structure, it is well-established that vibrations generated by the ground motion constitute the main limiting factors for reaching the luminosity of 10^{34} $cm^{-2}s^{-1}$. Several methods have been proposed to counteract this phenomena and active vibration controls based on the integration of mechatronic systems into the machine structure is probably one of the most promising. This paper studies the strategy of the vibration suppression. Active vibration control methods, such as optimized parameter of a numerical compensator, adaptive algorithm with real time control are investigated and implemented in the simulation layout. The requirement couldn't be achieved without the study of active-passive isolation able to damp high frequency ground motion. Thus, a pattern of a potential active/passive isolation has been proposed opening up prospects on the design of a future mechanical isolation.

1 INTRODUCTION

After the world's largest particle accelerator LHC (Virdee, T.S., 2010, *The LHC project*), the next generation of accelerators is being designed. Among them, the Compact Linear Collider CLIC is an ambitious project that proposes colliding beams of positrons and electrons.

The performance requirements of CLIC challenge the stabilization and control system in a number of areas. In order to achieve the required luminosity of 10^{34} $cm^{-2}s^{-1}$, two beams are accelerated and steered into collision. Considering the desired size of the beams (nanometer scale), the collision will require a very low vertical motion of these two beams all along the collider, and more specially through the last two focusing magnets. This can be done only by focusing and colliding the two separate beams to nanometer spot sizes. Thus, it imposes very tight constraints on the final focus (FF) system's alignment and stability.

The future CLIC composed of two arms of approximately 17 km long facing each other will accelerate beams at velocities near the speed of light. Once accelerated with the required energy and emittance (Assmann, R.W. et al., 28 July 2000) through the main linac, a sophisticated beam delivery system focuses the beam down to dimensions of 1 nm RMS size in the vertical plane and 40 nm horizontally. This requires the final focus magnets to be stabilized to vibration amplitude of

less than 0.1 nm for oscillations above 0.1 Hz at the interaction point (IP).

Given the tight specifications and hardware limitations, ground motion mitigation is a real challenge. This paper proposes a method to deal with ground vibrations. A first part aims to design a filtering algorithm combining feedback control and real time adaptive algorithm based on the generalized least square algorithm. Next a study of the global pattern of the isolation needed to achieve the requirements is presented. This paper ends up with numerical simulations and robustness test.

2 BEAM-BASED FEEDBACK

Once accelerated, the beam goes through a final focusing magnet subject to disturbances (see fig. 2) Stabilization of the beam can be obtained by using the corrective capabilities of the beam components by measuring the beam parameters (size, position…) tanks to a Beam Position Monitor (BPM) (not represented) and acting on the beam with a kicker. The frequency range in which this is possible is given by the beam repetition rate. For CLIC, this rate is 50Hz (which means that the beam is composed of a serial of trains separated from each other in time by 20 ms). This configuration imposes that the beam cannot be corrected above several Hz.

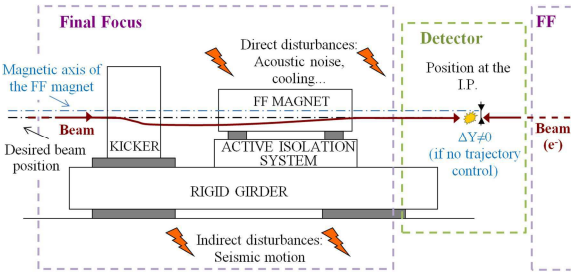

Figure 2: Final focus scheme.

As ground motion is still at a detrimental level until about 50-100Hz, depending on the site, it needs to be corrected by mechanical means. Thus, this magnet stands on an active-passive support designed to reduce ground motion vibrations.

The proposed control framework is composed of a feedback loop where the controller (*H*) defines the dynamical behaviour of the system. The structure of this control is given in figure 3 (The backward shift operator is denoted q^{-1}).

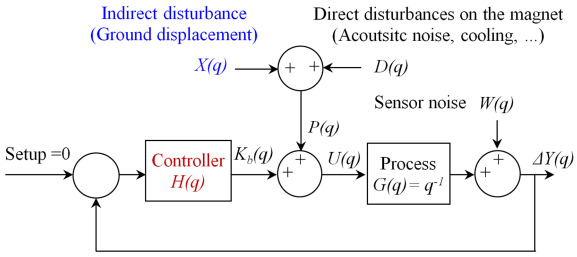

Figure 3: Scheme of the beam trajectory control.

The disturbance (*X*) is the mechanical excitation from ground motion (see part 2.1) which is also the disturbance felt by the magnets (Other sources of disturbances are neglected as their contribution to the beam motion is supposed to be insignificant compared to the ground motion itself). (*P*) is finally the disturbance felt by the magnet.

The transfer function between the mechanical displacement of this magnet and the beam can be modeled by a constant matrix (equal to 1 in the model as it is considered as a uniform rigid structure). Finally the noise of the sensor (*W*) is added to the displacement of the beam.

The action (K_b) meant to reduce the motion of the beam (or the offset between the two beams at the interaction point) is done by a kicker. The obtained displacement of the beam is proportional (equal to 1 in the following model) to the injected current of the kicker. The dynamic of the system is due to the frequency of the beam train, so the process can be treated as a first approach as a delay at a sampling period equal to 0.02 s.

This scheme allows to design a controller (*H*) that performs optimally (depending on the PSD of the ground motion) to minimize the integrated RMS displacement of the beam.

2.1 The ground motion

For this study, the reference is the measured motion in the tunnel of the Large Hadron (LHC) at CERN and more precisely, the ground motion where is located the Compact Muon Solenoid (CMS) calorimeter (The CMS Collaboration, 2008). Figure 4 represents the PSD and the integrated RMS of the ground motion measured at CMS thanks to a geophone (Güralp CMG-6T calibration: ±12.5 mm s-1, Frequency range: [0.033-50] Hz, sensitivity: 2x998 V s m^{-1}, resolution: 0.05 nm between 4 Hz and 50 Hz) (Güralp Systems Limited, Inc.)

Considering the limited bandwidth of the geophones, simulations have been computed in the frequency range [0.1-50] Hz instead of [0-∞[. Note that the limitation at 50 Hz has no impact on the

results as the PSD decreases significantly with frequency above this frequency.

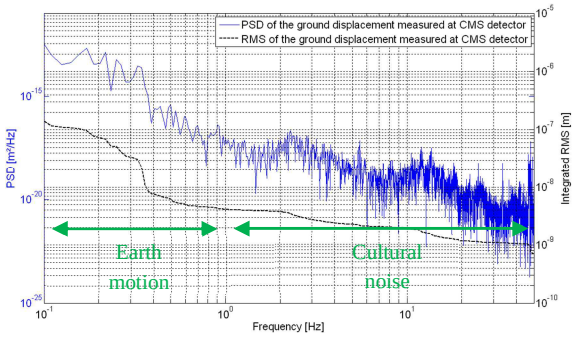

Figure 4: PSD and integrated RMS of the ground motion measured at CMS.

The PSD of the natural ground motion is a steep function of frequency which falls off as $1/f^4$. Several peaks can be observed, related to machinery and structural resonances. Such peaks appear as steps in the integrated R.M.S. PSD is particularly useful, because it allows to calculate the total RMS (Root Mean Square) displacement in any frequency band (or indeed over the whole frequency range measured) by integrating the displacement PSD and taking the square root.

2.2 Design of a classical controller

The required specifications impose to lower the integrated RMS(0). The controller has to provide real-time computation. Considering the process and the previous requirements, the structure of the controller has been chosen to be the following:

$$H(q) = \frac{b_0 + b_1 q^{-1} + b_2 q^{-2}}{1 + a_1 q^{-1} + a_2 q^{-2}}$$

Higher order structures of the controller have been tested but it didn't result in a significant gain compared to the complexity of the feedback control. Considering the previous scheme (fig.3), the closed loop transfer function taken into account is the transfer function between the beam displacement and the disturbance *X* (also called sensitivity transfer function):

$$F(q^{-1}) = \frac{\Delta Y}{X} = \frac{G}{1 + GH}$$

Note that as *G* is a pure delay, the effect, in term of amplitude of the closed loop on sensor's noise disturbance *W* (or any direct disturbance D) is the same as for the ground motion disturbance *P*.

2.3 Optimization of the controller

The method to lower the RMS(0.1Hz) of is the following:

- Estimation of the PSD of the measured ground motion signal ,
- Scanning the parameter space of the controller,
- For each of these combinations, if the parameters give a stable closed loop transfer function F, then:
- Computation of the PSD of the obtained output using:
- $PSD\big(Y(jw)\big) = |F(jw)|^2 . PSD(X(jw))$
- Computation of the integrated RMS ,
- Selection of the parameters' set of the controller that gives the minimum RMS(0).

As these parameters obviously depend on the PSD of the input disturbance (*P*), if this signal is changed in terms of PSD, then the optimization will produce another set of parameters.

The transfer function F between the ground motion disturbance and the output depends obviously on these parameters. In the optimized case, the next plot represents its transfer function:

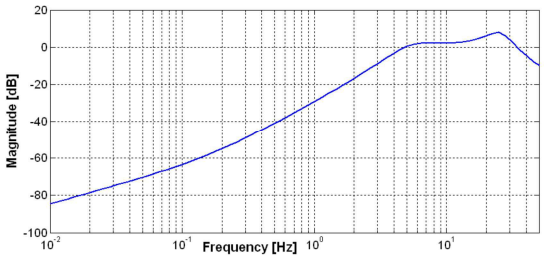

Figure 5: Sensitivity transfer function magnitude

However, the sensitivity transfer function F has an important property:

$$\int_0^{\omega/2} log|F(jw)|d\omega = 0 \quad \text{with} \quad \omega_e T_e = 2\pi$$

This formula obtained from Bode's sensitivity integral (Mohtadi, C., 1990, *Bode's integral theorem for discrete-time systems*) induces that lowering effects of disturbances at low frequencies will increase effects of disturbances at high frequencies (also called “water bed effect”).

2.4 Simulation results

The following simulation has been computed by injecting a sample of the ground motion disturbance. No other noise has been considered. Figures 6 and 7 represent the PSD and the integrated RMS

displacements obtained by simulation with the optimized feedback control loop:

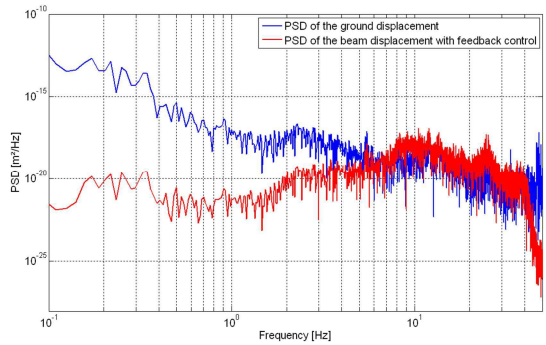

Figure 6: PSD obtained with feedback control

The plot above shows mainly two things; first of all, the controller is able to correct the beam trajectory to compensate effect of ground motion between [0-6] Hz. Then after 5-6 Hz, it will increase ground motion.

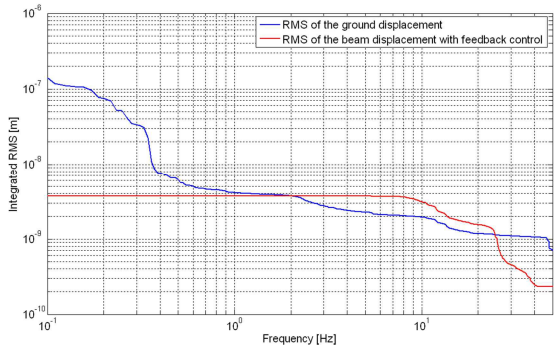

Figure 7: Integrated RMS obtained with feedback control

This amplification after 6 Hz has bad consequences for the integrated RMS which rises to almost 4 nm.

Because of the sample time of the process, the feedback is efficient in a very limited frequency bandwidth [0-5] Hz. It implies that the integrated RMS at 5 Hz of the disturbance *P* has to be the lowest possible, and that one cannot do better than this value by the means of a feedback control. It is thus necessary to consider a complementary solution able to filter the ground motion vibrations as much as possible. This study will be the topic of part 4.

3 FEEDBACK AND ADAPTIVE ALGORITHM STRATEGY

This strategy is most likely used when the sources of disturbances are unknown or variable in time, which is the case in this study. The dynamical behavior of the system is defined by the feedback loop, and an adaptive algorithm changes the command of the process to minimize the prediction error. The ordinary least-squares method may lead to biased or non-consistent estimates of system parameters in the presence of noise. The bias problem may be solved, for example, by using the generalized least-squares method. In the generalized least-squares method, a digital filter is used to filter the observed input-output data.

3.1 Design of the adaptive filter

The control scheme is the following:

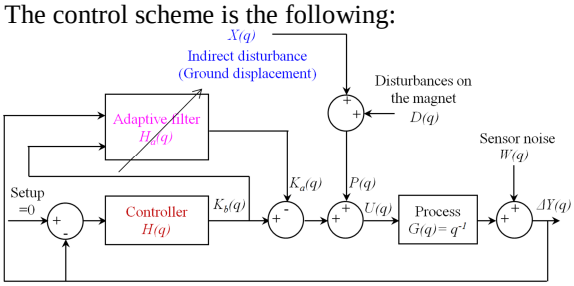

Figure 8: Adaptive feedback control scheme.

This control uses the prediction-error to reconstruct and cancel out the disturbance. This scheme is by nature non-linear as it is composed of two interlinked loops. To avoid such a complex study, a general adaptive command structure defined by Landau's stability theorem (Landau, I.D., Zito, G., 2006, *Digital Control Systems*) has been used. In practice the estimation scheme is needed to be iterative, allowing the estimated model to be updated at each sample interval as new data become available. The generalized least square algorithm estimates the parameters h of the filter H_a by minimizing the following least square criteria:

$$J(n) = \sum_{i=0}^{n} \lambda^{n-i}[e(n)]^2$$

This Algorithm uses the prediction error:

$$e(n) = Y(n) - \boldsymbol{K_b^T}(n)\boldsymbol{h}(n-1)$$

(balanced with a forgetting factor λ) made on the estimation to compute the next set of the parameters:

$$h(n) = h(n-1) + \boldsymbol{k}(n)e(n)$$

using the Kalman gain :

$$k(n) = \frac{\lambda^{-1}\boldsymbol{Q}(n-1)\boldsymbol{K_b}(n)}{1 + \lambda^{-1}\boldsymbol{K_b^T}(n)\boldsymbol{Q}(n-1)\boldsymbol{K_b}(n)}$$

and the Ricatti equation:

$$Q(n) = \lambda^{-1}\boldsymbol{Q}(n-1) - \lambda^{-1}\boldsymbol{k}(n)\boldsymbol{K_b^T}(n)\boldsymbol{Q}(n-1)$$

3.2 Simulation results

Figure 9 and 10 show the obtained performance using this configuration.

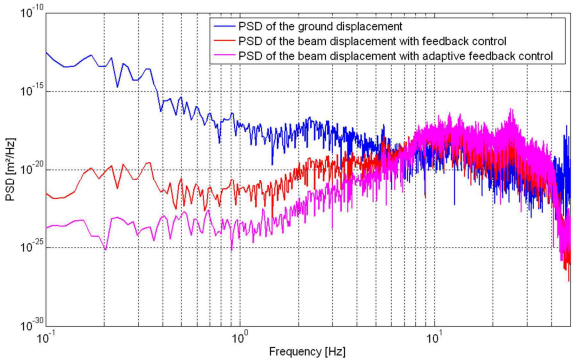

Figure 9: PSD obtained with adaptive feedback control.

The PSD plot shows that this adaptive scheme has allowed to considerably decrease the power of the ground motion displacement in the bandwidth [0-5] Hz. It also has the drawback to increase the amplification after 5 Hz leading to an integrated RMS worse than with feedback only.

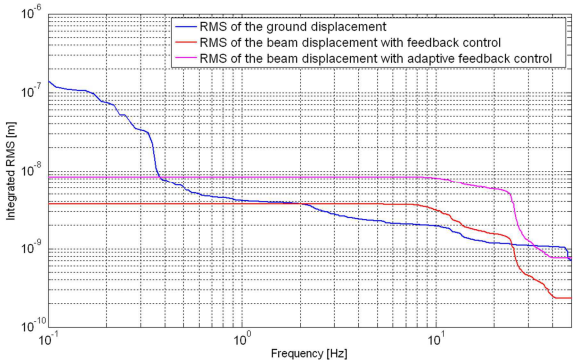

Figure 10: Integrated RMS obtained with feedback and adaptive control.

Previous observations with optimized feedback and adaptive control show that the residual integrated RMS displacement at 0.1 Hz of the beam displacement is mainly due to the integrated RMS at 5 Hz of the motion of the magnet support. Above that frequency, the control is not efficient. The strategy consists in adding active/passive isolation under the magnet which steers the beam. It has to attenuate the ground motion vibration from 5 Hz which means that the resonance frequency of this mechanical structure has to be below 5 Hz. Similar concepts have already been developed in the research and industrial field (Braccini, S. et al., 2005), (Ellison, J. et al., 2001, *Passive vibration control of airborne equipment using a circular steel ring*).

4 ACTIVE/PASSIVE ISOLATION

To avoid luminosity loss the vertical position of the magnets must be stabilized to 0.1 nm RMS for frequencies of 0.1 Hz and above. This will be achieved by the previous adaptive feedback controller and a passive pre-isolator, complemented by an active isolation system. The characteristic of this whole isolation system is determined by simulation in the next part.

4.1 Pattern of the mechanical support

This part aims to establish a pattern of the mechanical support needed between the ground and the beam to reach the specifications of 0.1 nm. This transfer function should be representative of a typical mechanical support dynamical behavior. Thus, it has been modeled by the following 2nd order low-pass filter:

$$K_g(s) = \frac{G_0}{1 + \frac{2\xi}{\omega_0}s + \frac{1}{\omega_0^2}s^2} \qquad \text{with } \omega_0 = 2\pi f_0$$

This scheme implied to optimize the controller for each combination (f_0, G_0), until an eventual solution allows to reach the specifications (The mechanical filter modification imply a modification of the input disturbance *(P)* and a re-optimization of the controller, see part 3.2). The body of the combinations (f_0, G_0), see figure 11, constitutes the pattern of the desired active-passive isolation dynamic.

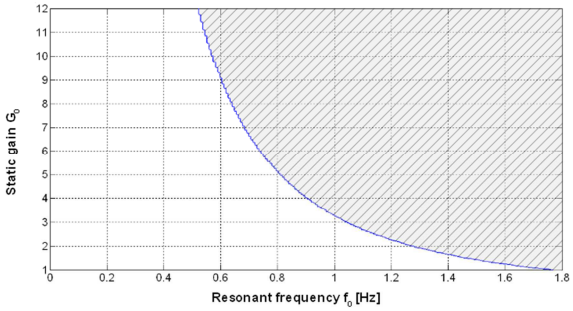

Figure 11: Pattern of the active-passive isolation dynamic.

The area under the curve represents the body of the combinations (f_0, G_0). The simulation showed

that this pattern is independent of the damping ratio ξ in the range [0.005 0.7]. This results from the extremely high efficiency of the adaptive feedback control in low frequencies.

This pattern is actually used for a more detailed study of a mechanical support design. This support will be efficient enough to achieve the desired performances.

4.2 Passive isolation

The ground micro-seismic motion at frequencies above 4 Hz, either natural or generated by machinery, can be effectively reduced by a passive mechanical low-pass filter currently being designed (Ramos, F., *Dynamic analysis of the FF magnets pre-isolator and support system*). In this scheme, the whole system sits on a big massive support; the pre-isolator:

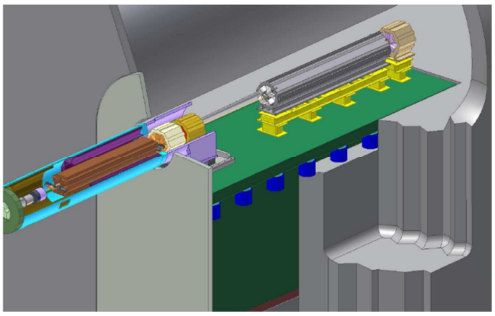

Figure 12: Layout of the pre-isolator, with the concrete mass supporting the two final focus magnets

The two magnets are supported by rigid girders that are fixed on top of a massive concrete block, weighing about 80 tons and resting on several springs (in blue in Figure 12) whose rigidity is tuned in order to have a vertical resonance of the whole assembly at 1 Hz. The transfer function of this mechanical filter is given figure 13:

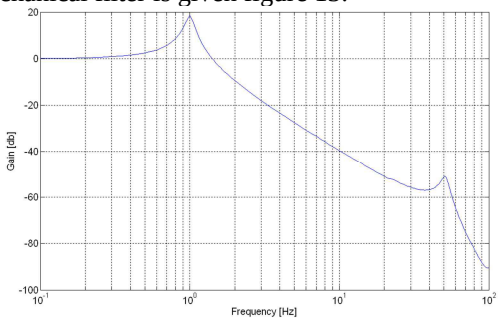

Figure 13: Transfer function of the pre-isolator.

Ground motions at frequencies above 1 Hz are reduced by a factor f^2 up to the first internal resonant mode, which can be tuned to be in the bandwidth 30 – 50 Hz. The system is designed to provide a reduction of the RMS vertical displacement from about 3 to 0.1 nm at 4 Hz and it has to work in combination with the active stabilization (i.e. adaptive feedback control plus an eventual combination with an active/passive isolation).

4.3 Mechanical support consideration

The study of the design of such an active support is not the topic of this paper. Its behavior (described part 4.2) has been modelised by a product of two second-order low-pass filters (K_1 and K_2, $K=K_1.K_2$) with resonance frequencies f_1 = 1 Hz and f_2 = 50 Hz and damping ratios ξ_1 = 0.05 and ξ_2 = 0.075.

$$K_{1,2}(s) = \frac{1}{1 + \frac{2\xi_{1,2}}{\omega_{1,2}} s + \frac{1}{\omega_{1,2}^2} s^2} \qquad \text{with } \omega_0 = 2\pi f_0$$

This dynamic has been implemented in the next simulations (see figure 14)

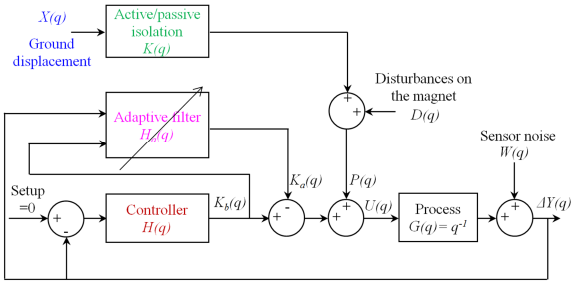

Figure 14: Feedback and adaptive control scheme with active/passive isolation simulation.

4.4 Results

The following plots represent the simulation results of the feedback and adaptive control obtained when filtering the ground motion by the pre-isolator's transfer function.

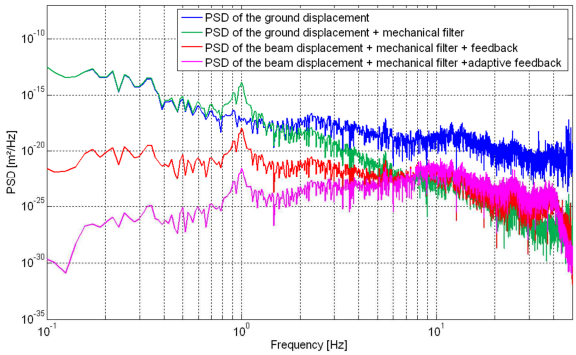

Figure 15: PSD obtained with adaptive feedback control and mechanical filter.

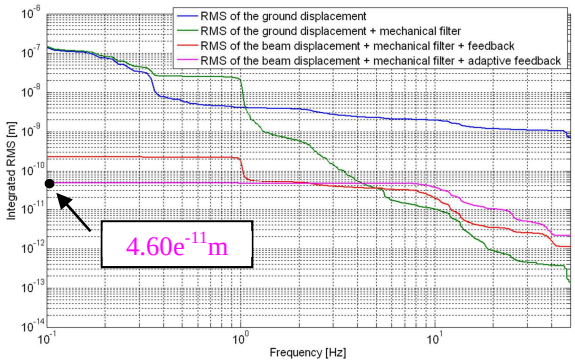

Figure 16: Integrated RMS obtained with adaptive feedback control and pre-isolator.

The simulation shows that this strategy combining passive isolation to damp fast motion of the ground and feedback loop coupled with an adaptive algorithm which deals with slower motions is able to reach an integrated RMS at 0.1 Hz of $4.60e^{-11}$ m.

The previous study is based on a model of the real system currently under development. Considering the current project status, it was thus necessary to make several assumptions and to arbitrarily fix certain parameters.

4.5 Robustness

The goal here was to observe the influence of the sensor's noise on the control's behavior. Figure 17 shows the variation of the integrated RMS displacement of the beam versus the noise of the BPM (represented by a white noise (*W*) added to the measured displacement).

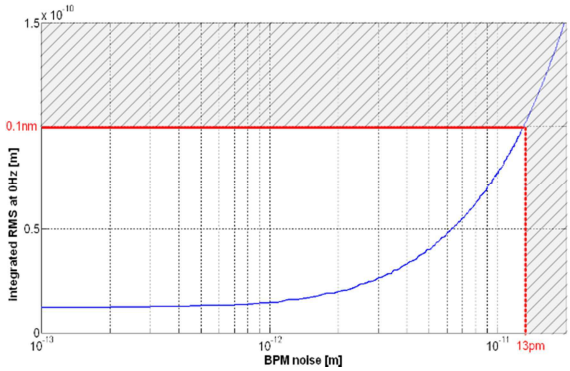

Figure 17: Variation of the integrated RMS displacement at 0.1 Hz versus BPM noise.

The level of sensor's noise is crucial for a good performance of the control. It cannot exceed 13 pm integrated at 0.1 Hz to respect the specifications. As the BPM gives an indirect measurement (amplified image of the position by 10^5), the BPM's noise has to be < 1.3 µm integrated RMS @ 0.1 Hz. This result has to be taken into consideration in the design of this monitor and will certainly be one of the strategic requirements.

4.6 Perspective

Previous results could even be improved by combining the previous passive isolation with active isolation systems. A study of the different commercial solutions (Redaelli, S., 2003, Thesis) aimed to select the most efficient one on the market for this type of application. The selected solution is a TMC table with STACIS feet (TMC Company, 2002), also described in (Geffroy, N. et al, Mechatronics 2008), see figure 18:

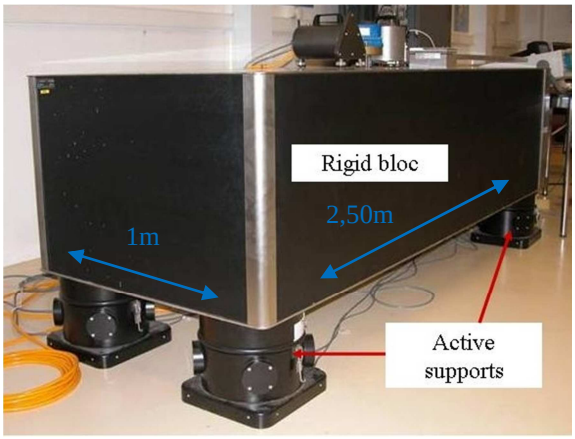

Figure 18: TMC table with STACIS feet.

This product is able to manage vibrations at a sub nanometer scale. However, given the tight tolerances, and the cost of such a product, a dedicated solution is being developed. This system includes four piezoelectric actuators and four capacitive sensors. Such a system is potentially suitable to be handled by three degrees of freedom algorithm controlling the vertical motion and the two associated rotations.

5 CONCLUSIONS

In this paper we have presented our methodology of the stabilization of the future Compact Linear Collider. Considering that the imposed tolerances

(integrated RMS(0.1) at the interaction point has to be lower than 0.1 nm) are considerably lower than the natural ground motion (a few micrometers), these requirements are very challenging and were never achieved in the past. This article has represented a mechanical setup and a dedicated control approach which allows to obtain a very low vertical displacement of the beam at the interaction point of about an integrated RMS(0.1) of 0.046 nm. In order to perform these results, the strategy was to carry out a study on an innovative control which is very efficient in low frequencies. This algorithm is composed of a combination of a feedback obtained thanks to a parametric study and an adaptive control based on the generalized least-squares method. This method was tested in simulation with a representative model of the system and with real measurement of the ground motion. Next, a pattern of the dynamic of the required mechanical damping structure, needed to filter the vibrations above a few Hertz has been established for the purpose of a further development. To validate this study, simulation test with a mechanical support have been performed, and robustness tests as well in order to take into account the prediction errors of the mechanical system model and to estimate the acceptable maximal sensor noise. The study opens up perspectives for the construction of an active-passive isolation support as well. Thus, a massive support is currently being studied and a dedicated active isolation integrating vibration sensors, piezoelectric actuators and an appropriate instrumentation is being designed.

6 ACKNOWLEDGMENT

The research leading to these results has received funding from the European Commission under the FP7 Research Infrastructures project EuCARD, grant agreement no.227579. The authors wish to express their thanks to D. Schulte, J. Pfingstner and K. Artoos from C.E.R.N., for this project and fruitful collaboration.

REFERENCES

Virdee, T.S., 2010, *The LHC project: The accelerator and the experiments*, Nuclear Instruments and Methods in Physics Research A, doi:10.1016/j.nima.2010.02.142.

The CMS Collaboration, 2008, *The CMS experiment at the CERN LHC*, Journal of Instrumentation.

Assmann, R.W. et al., 28 July 2000, *A 3 TeV e+ e– Linear Collider Based on CLIC Technology*, CERN European Organization for Nuclear Research.

Goldman, S., 1999**.** *Vibration Spectrum Analysis*, Industrial Press, ISBN 978-0-8311-3088-6.

Güralp Systems Limited, Inc.

Mohtadi, C., 1990, *Bode's integral theorem for discrete-time systems*, IEE proceedings. Part D. Control theory and applications vol. 137, no2, pp. 57-66.

Landau, I.D., Zito, G., 2006, *Digital Control Systems: Design, Identification and Implementation*, Communications and Control Engineering.

Ellison, J. et al., 2001, *Passive vibration control of airborne equipment using a circular steel ring*, Journal of Sound and Vibration, Volume 246, Issue 1, Pages 1-28.

Ramos, F., *Dynamic analysis of the FF magnets pre-isolator and support system*, to be published.

Braccini, S. et al., 2005, *Measurement of the seismic attenuation performance of the VIRGO Superattenuator*, Astroparticle Physics 23 557–565.

TMC Company, 2002, *TMC STATIS 2000 Stable Active Control Isolation System*, User's manual, Document P/N 96- 26690-02 Rev. D.

Geffroy, N., Brunetti, L., Bolzon, B., Jeremie, A., Caron, B., Lottin, J., *Active stabilization studies at the sub-nanometer level for future linear colliders.* Mechatronics 2008.

Redaelli, S., 2003, *Stabilization of Nanometer-Size Particle Beams in the Final Focus System of the Compact LInear Collider (CLIC)*, Thesis, Lausanne.